W,Z° PRODUCTION AT A PP COLLIDER

G. Bunce, H.A. Gordon, T.J. Killian, M.J. Murtagh, F.E. Paige, M.J. Tannenbaum, T.L. Trueman
Brookhaven National Laboratory, Upton, NY 11973

J. Branson
Massachusetts Institute of Technology, Cambridge, MA 02139

F. Eisler
College of Staten Island, Staten Island, NY 11301

P. Grannis
State University of New York at Stony Brook, Stony Brook, NY 11794

I. W,Z° Production at a pp Collider

Introduction

We have examined some experimental questions relating to the production of W's and Z°'s at a pp collider. To be specific we have considered a Colliding Beam Accelerator (CBA) with center of mass energy $\sqrt{s}$ = 800 GeV and luminosity $L = 10^{33}cm^{-2}sec^{-1}$ (the standard BNL Isabelle (ISA) operating conditions). Most experiments should accumulate 10^7 sec of beam and therefore will have an integrated luminosity $L = 10^{40}cm^{-2}$. This corresponds to the production of millions of conventional charged W's per interaction region and gives the potential for high statistics studies of the properties of W's and for experiments searching for higher mass objects.

Our focus has been on testing predictions of the standard model. We have concentrated on W production since it is likely the standard Z° will be observed in the near future. In most cases the W is detected via its semileptonic decay $W \to \ell + \nu$. Detailed studies[1] by the MIT group have established the feasibility of a muon detector for the study of W, via its muon decay $W \to \mu + \nu$, which could operate at $L = 10^{33}cm^{-2}sec^{-1}$. In section 5 we consider the possible limitations of this detector at even higher luminosities $L = 10^{34}cm^{-2}sec^{-1}$. However for most other topics we have investigated the W using its electron decay $W \to e + \nu$ as a signature. The open geometry required in this case is more appropriate for experiments investigating details of W production or electroweak phenomena such as $pp \to W^{\pm} + \gamma + X$, π^0 or single photon production.

Since we wish to focus on rates and on the effectiveness of topological cuts we have to consider a schematic detector. The detector is assumed to cover $\Delta y = \pm 2$ (i.e. a 15° beam cone is excluded) and $\Delta\phi = 2\pi$. It has electromagnetic and hadronic calorimeters. They are segmented in towers pointing to the interaction diamond. Each tower covers 5° in Θ and 9° in ϕ. We have assumed an electron identification system (e.g. transition radiation detector) which gives $\pi/e \approx 1/1000$ in a test beam or $\approx 1/100$ π rejection in the experiments discussed here. The detector is assumed to have a magnetic field so that at least the signs of the leptons can be determined. However, at present, the particles are not tracked in the field but are projected directly from the interaction point to the detector. Where detailed studies of the rates and backgrounds were made we used appropriate event sets generated by the ISAJET[2] Monte Carlo program. In general it is easy to generate adequate signal events. However for integrated luminosity $\approx 10^{40}cm^{-2}$ the generation of adequate background events is not trivial as one is usually dealing with the tails of distributions.

The specific topics considered are outlined here and discussed in more detail in the following sections:

a) $W^{\pm}$ production: $pp \to W^{\pm} + X$, $W^{\pm} \to e^{\pm} + \nu$

The $W^{\pm}$ cross section is $3.5 \times 10^{-33}cm^2$ for W^+ ($1.6\times10^{-33}cm^2$ for W^-) at $\sqrt{s}$ = 800 GeV.[3] Since the $W^{\pm} \to e^{\pm}\nu$ branching ratio is calculated to be 8.5%, a total of 3×10^6 W^+ ($1.4\times10^6 W^-$) semileptonic $W^{\pm}$ decays are detectable in an experiment with an integrated luminosity of $10^{40}cm^{-2}$. We have considered (Section II) the feasibility of doing this experiment and the mass resolution on the $W^{\pm}$ one might finally attain. Running at $L = 10^{33}cm^{-2}sec^{-1}$ is not a problem. The trigger rate for a reasonable lepton P_T cut ($P_T \gtrsim 20$ GeV/c) can easily be reduced to less than 1 per second. The pile up due to event overlap during the calorimeter collection time ($\approx$ 200 nsecs) does not seriously affect the topological cut required to reduce the contributions to the high P_T electron signal from semileptonic heavy quark decays. Furthermore if one assumes that after analysis the region with $P_T > 25$ GeV/c is essentially background free and that the Z° and W have identical P_T distributions, the W mass will be determined to an accuracy of .5 GeV to 1 GeV.

b) $pp \to W^{\pm} + \gamma + X$

The processes $pp \to W^{\pm} + \gamma + X$ and $pp \to W^+ + W^- + X$ are important to study as they give measurements of the fundamental trilinear self couplings which are present in any gauge group structure. We have considered (Section III) the reaction $pp \to W^{\pm} + \gamma + X$. The cross section for this process has been calculated[4] for $P(\gamma)>5$ GeV/c to be $\approx 4\times10^{-35}cm^{-2}$ at $\sqrt{s}$ = 800 GeV. However it is a steep function of the transverse momentum of the photon ($P_T(\gamma)$), falling to $\approx 4\times10^{-36}cm^2$ for $P_T(\gamma) > 10$ GeV/c. If the $W^{\pm}$ is detected via its leptonic decay $BR(W^{\pm} \to e^{\pm}\nu) = 0.085$, then ≈ 2700 $pp \to W^{\pm} + \gamma + X$, $W^{\pm} \to e^{\pm}\nu$ events will be observed in an experiment with integrated luminosity $L = 10^{40}cm^{-2}$. The major physics background is from the process $pp \to W^{\pm}$ + (high P_T jet) where the jet fragments include a high P_T π^0. In the appropriate P_T interval this latter cross section is ≈ 240 times the $pp \to W^{\pm} + \gamma + X$ cross section. This background can be significantly reduced by simple topological constraints on the energy deposition around the apparent single photon shower in the jet events. This preliminary study shows that it is quite straightforward to get a signal to background ratio of one to one.

c) Polarization effects in $W^{\pm}$ production

The AGS at Brookhaven will soon be running with a polarized proton beam. This can be transported to the CBA to give a colliding polarized beams option. There

is every expectation (Section IV) that one can attain the same luminosity for polarized beams as for unpolarized beams. A high luminosity polarized proton collider would be very useful in studying weak interaction effects. We have considered the problem of measuring the reaction $W \to Q\bar{Q}$ jets. The $Q\bar{Q}$ effective mass distribution from QCD processes is ≈ 50-100 times the $W \to Q\bar{Q}$ signal in the region of the W mass.[5] Without polarized beams it is difficult to see how, even with very high statistics, one could reliably parameterize the steeply falling background distribution to extract the signal. On the other hand, the use of polarized beams does afford a reliable background subtraction. The QCD background would be the same for positive and negative helicity running, while for 70% polarization $\sigma_-(pp \to W^+) \simeq 2\sigma_+(pp \to W^+)$, where $\sigma_-(\sigma_+)$ is the cross section for left (right) handed polarized protons. Consequently a straightforward bin by bin subtraction of the $Q\bar{Q}$ effective mass distributions can be performed to obtain the $W \to Q\bar{Q}$ signal.

If the standard model is not correct, polarized beams could be very important for trying to determine the handedness of the new W's.

d) Very high luminosity experiments

Detectors which emphasize muon detection are not rate limited at $L = 10^{33}\,cm^{-2}sec^{-1}$. We have considered the potential of this type of detector (Section V) for luminosities of $\approx 10^{34}\,cm^{-2}sec^{-1}$. Most of the interesting physics requiring very high luminosity can be done. The muon trigger rate at high P_T is not limited by the singles rate. Consequently searches for $\mu^+\mu^-$ decays of heavy neutral objects and the observation of heavy charged bosons via their semi-leptonic decay ($W^+ \to \mu^+\nu$) are feasible. At this luminosity the effectiveness of a calorimeter system for imposing topological cuts is greatly reduced. However, the study of very high P_T jets ($P_T > 150$ GeV/c) should be possible and should not be effected by pile up.

In non-standard models there are multiple Z°'s with undetermined couplings and model dependent cross sections and widths. We have quantified the sensitivity of this high luminosity CBA $\int Ldt = 10^{41}\,cm^{-2}$ to higher mass Z°'s. Under simple assumptions on the mass dependence of the cross section we find that at the level of 100 events per 10^7 sec experiment one can detect $Z^\circ \to \mu^+\mu^-$ masses up to 320 GeV.

II. W^+ Production

Introduction

We have considered an experiment to observe the W^+ via its decay $W^+ \to e^+\nu$ and to determine its mass from the e^+ transverse momentum distribution. A generic open-geometry detector which provides charged-particle tracking in addition to hadronic and electromagnetic calorimetry was used. We have concentrated mainly on the characteristics of the calorimeter, which we assume to be uniformly sensitive over the entire solid angle, with the exception of 15 degree cones in the forward and backward hemispheres. This reduces the very large triggering rate from beam-jet events. The calorimeter is divided into cells 5° in polar angle by 9° in azimuth. This corresponds to roughly one cell per unit of rapidity in the forward direction, with increasingly finer rapidity coverage at wide angles.

The calorimeter is segmented radially into an electromagnetic and a hadronic part, so that the readout (per cell) consists of an electromagnetic energy and a total energy. We have not considered such refinements as position interpolation on the face of the cell, energy resolution or hadronic energy deposition in the electromagnetic calorimeter. We have supposed that the track chambers provide reasonably good momentum resolution (a few percent at 10 GeV), but in most of the discussion which follows, only the charge information is used. Charged particles with momentum less than 300 MeV/c were assumed to be trapped by the magnetic field and they were not used in the calculations of deposited energy.

Trigger Rate

The primary trigger for this experiment is an energetic electromagnetic shower. Additions to this will be necessary. For example, one could require that at least (or only one) charged particle point into the triggered tower, that there was an electron (identified by using the transition radiation detector) pointing near the triggered tower, or ultimately that the entry point of the charged particle in the tower and the shower origin were consistent to a few cms. To apply these more complex topological components of the trigger, it is important that the primary trigger rate not be too high.

The dominant source of electromagnetic showers is not electrons but π°'s. We have calculated for $L = 10^{33}\,cm^{-2}sec^{-1}$ the π° induced trigger rate per second for a detector with acceptance $\Delta y = \pm 2$, $\Delta\phi = 2\pi$ ($\Delta y \Delta\phi = 8\pi$). The ISR π° data for large P_T ($P_T > 7.5$ GeV/c) is well described by the CCOR fit

$$\sigma_{INV} \equiv E\frac{d^3\sigma}{dp^3} = 4 \times 10^{-29}\,\frac{(1-X_T)^{12}}{P_T^{5}} \quad .$$

The expected $P_T\,\sigma_{INV}$ rate as a function of P_T for π°'s at $\sqrt{s} = 800$ GeV determined from this fit is shown in Fig. 1. At large P_T it is quite consistent with the results of Owens, Reya and Gluck.[6] At lower P_T the theoretical calculation gives a significantly steeper P_T dependence. Preliminary measurements from the CERN $\bar{p}p$ collider support the theoretical low P_T behavior.[7] In the P_T range $14 \le P_T \le 120$ GeV/c the function σ_{INV} can be well parameterized by the form

$$\sigma_{INV} \equiv F(P_T) = \frac{A}{P_T^{\,n}}$$

with $n = 8.1$ and $A = 1.55 \times 10^{-24}$. The number of π° triggers per second with $P_T' > P_T$, $N_T(P_T)$, is then given by

$$N_T(P_T) = L\,dy d\phi \int_{P_T}^{\infty} P_T'\,F(P_T')\,dP_T'$$

$$= 8\pi\,\frac{LP_T^2}{(n-2)}\,F(P_T)$$

The resulting primary trigger rates as a function of P_T are shown in Table I. For $P_T > 20$ GeV/c one has 120 triggers per second.

TABLE I.
Trigger rate from π°'s at L = 10^{33} cm^{-2} sec^{-1}

P_T(GeV/c)	Triggers per Sec.
> 10	5000
16	380
20	120
30	8.9
40	1.1
60	0.11
80	0.02
100	0.005

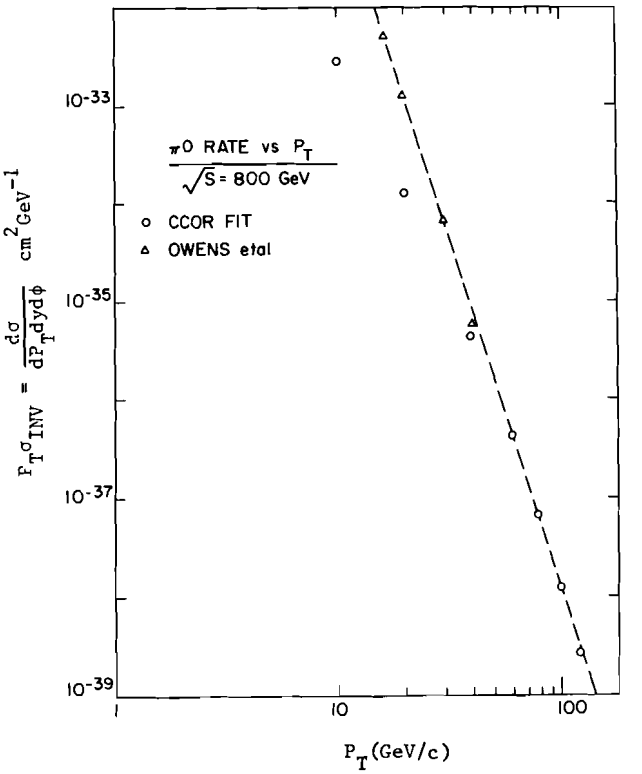

Fig. 1. The π° rate as a function of transverse momentum.

For $P_T(\pi^\circ)$ > 10 GeV/c only 10% of the triggered towers will have at least one positive charged track pointing into them. Furthermore since the typical charged multiplicity in any tower around the triggered tower is ≈ 1, even a crudely segmented transition radiation system will give another factor of ≈ 100 reduction in the trigger rate from π°'s. Consequently one can easily envisage a final trigger rate for π°'s with charged hadron overlaps of 10^{-3} of the primary trigger rate.

The $(\pi^+ + \pi^-)$ rate is double the π° rate. At most 1% of the charged pions will produce a shower in the electromagnetic calorimeter which is not distinguishable from a purely electromagnetic shower. The additional factor of ≈ 100 reduction achieved from the transition radiation reduces the charged pion trigger rate to ≈ 10^{-4} of the primary π° trigger rate.

Dalitz decays and early conversions are non-trivial sources of real electron triggers. With the simple parameterization of the π° spectrum given above, one analytically calculates the number of $e^\pm$ relative to π° with $P'_T > P_T$ to be

$$\frac{e^+ + e^-}{\pi^\circ} = \frac{2}{(n-1)^2}(2t + \delta)$$

where δ = 0.012 is the π° Dalitz branching ratio and t is the thickness of material (mostly vacuum chamber) in percent of a conversion length. For t = 1.5% and n = 8.1

$$\frac{e^+ + e^-}{\pi^\circ} = 1.7 \times 10^{-3} .$$

The final triggering rate will, therefore, probably be dominated by the $e^\pm$ from Dalitz decays and conversions.

High P_T e^+ Sources

We considered four different sources contributing to the high P_T single positron spectrum: the W^+ decays themselves; Z° decays with only the positron detected; semileptonic decays of heavy quarks; ordinary two-jet events. The last category is predominantly light quark jets producing π°'s which either fake an electron signal or undergo Dalitz decay. For each of these sources, we have plotted the P_T spectrum as measured by the (electromagnetic) calorimeter, for cases in which the calorimeter cell has a single positive track pointing to it.

The solid curve in Fig. 2 is the sought-for $W^+ \to e^+\nu$ signal. For comparison, the e^+ spectrum from $Z^\circ \to e^+e^-$ where both the e^+ and e^- are detected is shown as the dashed curve; this is not a significant background, however, since most of the time the e^- is detected as well. If one rejects events in which there is an observed e^+e^- pair with mass above 40 GeV, the Z° background is reduced to the dashed-dot curve.

The other curves represent the background from semileptonic decays of heavy quarks. The upper curve is for events selected as described above. If one makes the additional requirement that the charged track entering the calorimeter cell has a momentum of at least 95% of the calorimeter energy, one loses half the events, and the curve drops as shown. Additional rejection of heavy quark decays may be obtained by rejecting events in which the transverse momentum in the towers surrounding the triggered electron towers is large. Previous estimates of this effect give rejection factors of as much as 10 for heavy quark decays.[8]

The dominant background is from light quarks jets giving high P_T π°'s with a charged track overlap. The rate for a π° with a single positively charged track pointing into the cell is approximately 1000 times the W^+ signal even at moderate transverse momentum (P_T ≈ 20 GeV/c) as indicated in Fig. 3. The transition radiation system should give an additional 100/1 rejection of charged hadrons. In addition another order of magnitude is gained by requiring that the shower energy and hadron track momentum are consistent (E/P > 95%). If one requires no charged tracks in the eight cells surrounding the electron, an additional factor of two is obtained, with a corresponding loss of only 10% in the W^+ signal. Further reduction in this background comes from requiring the entry point of the charged track to be coincident with the shower origin and that there be a single shower and not two distinguishable showers from the π°. It seems quite reasonable to obtain the factor of 1000 reduction required to have the background of fake positrons from π° with charged hadron overlap less than the $W^+ \to e^+\nu$ signal above P_T of 20 GeV/c.

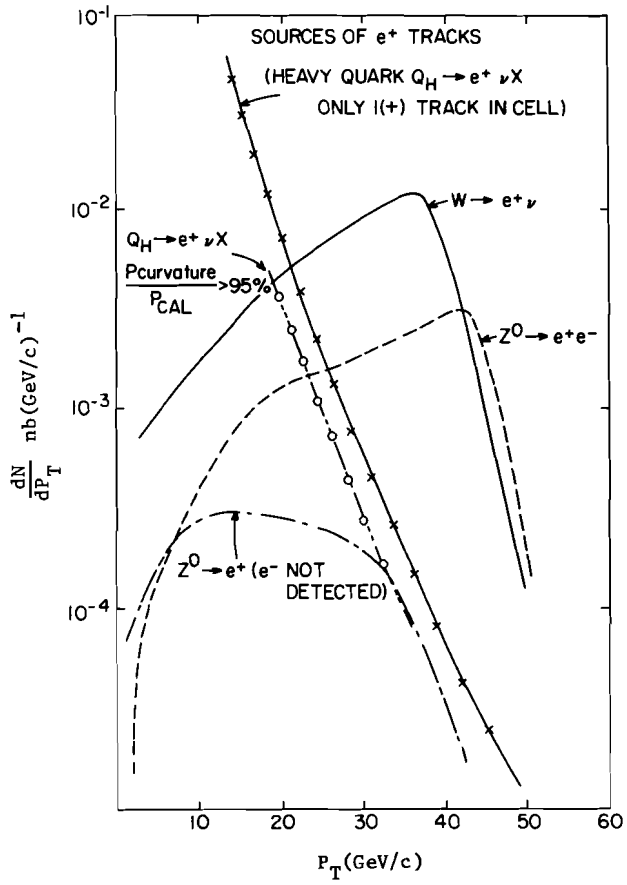

Fig. 2. Sources of high P_T positrons.

In the trigger section the rate for positrons from Dalitz decays was calculated to be $\approx 1 \times 10^{-3}$ of the π° rate. Further reductions in this background are less obvious. Requiring no tracks in the surrounding cells and no additional separable electromagnetic showers in the trigger cell will give approximately a factor of five reduction.

In general it appears straightforward to reduce the backgrounds of single positrons so that the W^+ contribution to the high P_T single positron spectrum is dominant above P_T of 20 GeV/c. We have not considered transverse momentum balance in the above discussion. In principle the $W^+ \rightarrow e^+\nu$ events have large missing transverse momentum carried by the neutrinos while most of the backgrounds have none (or less missing P_T in the case of heavy quark decays). This should provide additional background rejection and will probably be most useful in reducing the background from Dalitz decays.

It is important to note that there is negligible background from pile-up events. This is because the minimum bias events which pile up have essentially no particles at appreciable transverse momentum, and the chance of getting more than a few GeV in a particular small solid angle is vanishingly small. This contrasts with a total-energy trigger, where the solid angle is large, and no correlation is demanded among the particles which make up the energy sum.

Determination of $W^\pm$ Mass from the Electron P_T Distribution

We have considered how well one can determine the $Z, W^\pm$ mass difference from a high statistics measurement of the electron P_T distribution. The basic philosophy used is as follows: the Z° events in which both the e^+ and e^- are detected can be used both to determine the P_T shape of the Z° production and, by ignoring the e^- track from these events, the P_T distribution for $Z^\circ \rightarrow e^+$ (e^-).

This P_T distribution depends upon the details of the transverse and longitudinal momentum dependences of the colliding partons in some complicated way. Because Z°'s are produced from $u\bar{u}$ and $d\bar{d}$ collisions and $W^\pm$ from $\bar{u}d$ and $d\bar{u}$ collisions, the P_T dependences of Z° and $W^\pm$ are expected to be similar. Differences in the decay single $e^\pm$ distributions due to the mass difference, polarization effects or fine details of the u or d structure functions are expected to be small and calculable. Thus the P_T distribution observed for $Z^\circ \rightarrow e^\pm$ (with the Z° tagged by observing the other electron) can be used to compare with the observed P_T distribution for $W^\pm \rightarrow e^\pm\nu$. Loosely, we imagine scaling the measured Z° P_T spectrum down until it agrees with the spectrum from the $W^\pm$ signal.

The precision with which $\Delta M = M_Z - M_W$ can be measured depends on (a) statistics, (b) differences in background contamination for Z° and W, (c) uncertainty in the Z°,W production distributions which may arise from differences in the quark structure functions, and (d) the sharpness of the Jacobean peak. The backgrounds shown in Fig. 2 for the trigger level suggest that above $P_T \approx 25$ GeV/c the signal to ratio background exceeds 10. Analysis cuts involving shower shape requirements, missing P_T (carried by the neutrino) and additional topological constraints against jets will further improve the background rejection. Consequently we expect negligible background above 25 GeV/c for both W and Z°. As discussed above, intrinsic differences in Z°,W production should be small since $m(W)/m(Z^\circ) \approx 0.9$.

To approximate the procedure described above, six Monte Carlo experiments for different mass values (M = 81.0, 81.5, 82.0, 82.5, 83.0 and 84.0 GeV) were performed. The $W^\pm$ invariant cross-section was taken to be constant for $P_T < 1$ GeV/c, inversely proportional to P_T^2 for $P_T > 1$ GeV/c with $\langle P_T^2 \rangle = 100 (\text{GeV/c})^2$. This is consistent with many estimates of boson production, but it gives a factor of two sharper fall-off of the large P_T tail of the Jacobean peak than the most pessimistic calculation.[9] In each case the mass was taken to be a Breit-Wigner with mass M and width 3 GeV, and 5×10^4 events were generated. This is 6 times fewer W^+ events than one would realize in the detector discussed above for an experiment with integrated luminosity of 10^{39} cm^{-2}. However, it is comparable to the expected Z° event sample which will be the statistical limit. The generated P_T distributions for two selected masses are shown in Fig. 4. One can now consider the P_T distribution for one mass (M_l) to be the experimental data and other distributions for masses M_k, k = 2, 6 to be the expected W^+ distributions calculated from the measured $Z^\circ \rightarrow e^+$ distribution. The question then is how close in mass ($M_l - M_k$) two distributions can be before they are indistinguishable. To quantify this, a χ^2 is calculated:

$$\chi^2 = \frac{1}{N_D} \sum_{P_T > 25 \text{ GeV/c}} \frac{[N(M_l, P_T) - N(M_k, P_T)]^2}{\sigma^2}$$

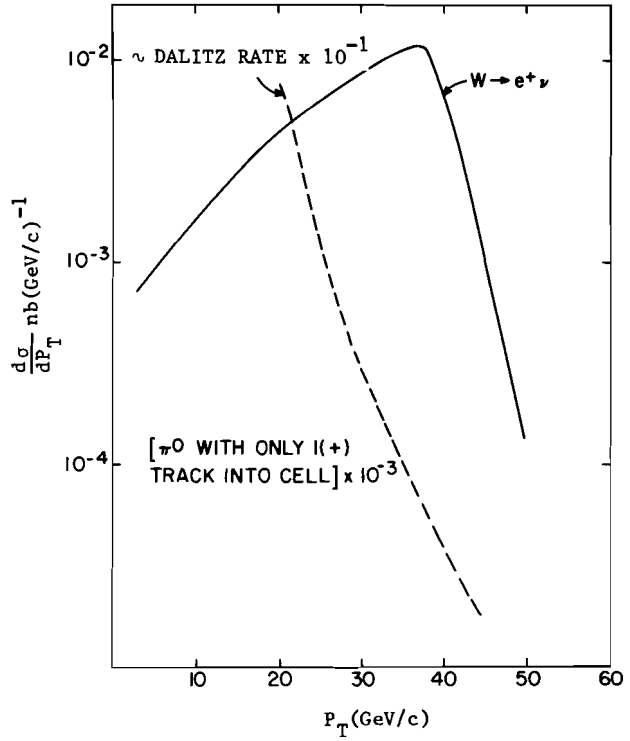

Fig. 3. High P_T e^+ distribution from a) $W^+ \to e^+\nu$ and b) π^0 + hadron overlap in jet events.

where only data above P_T = 25 GeV/c is used, N_D is the number of degrees of freedom and $\sigma = [N(M_l) + N(M_k)]^{1/2}$. This χ^2 is calculated for each pair of mass distributions. Fig. 5 shows χ^2 versus $\delta M = M_l - M_k$ for the cases $|y_e| \leq 1, 1 \leq |y_e| \leq 2$ and all y_e. The distribution of χ^2 versus δM is by definition symmetric around $\delta M = 0$ so for clarity only one branch of each curve is plotted. The curves all appear consistent with $\chi^2 \propto (\delta M)^2$ and since the error in mass is set by $\chi^2 = 1$ we find

$\delta M = 0.3$ GeV from all events
$\delta M = 0.5$ GeV from events with $y_e + < 1$
$\delta M = 0.55$ GeV from events with $1 < y_e + \leq 2$.

These errors are of course statistical only, although they were deduced assuming only a fraction of the $W^{\pm}$ events were useful for analysis after cuts against backgrounds. Enlargement of these errors by a factor of two is required if the rather broad P_T distributions of Halzen, Martin and Scott[9] are adopted. However in this rather detailed calculation, including recent structure function and polarization effects, we do observe that the shape of the electron spectra from Z° and W are similar to a high degree.

Our conclusion is that the difference in mass between Z° and W can probably be measured in pp colliders to a precision of 0.5 GeV to 1 GeV, in a way that is free from most sources of theoretical and experimental systematic errors. At this level of accuracy, the tests of the standard model become rather stringent, enabling one to probe for deviations from the standard model and search for evidence of new phenomena.

III. $pp \to W^{\pm} + \gamma + X$

The reactions $pp \to W^{\pm} + \gamma + X$ and $pp \to W^+ + W^-$ + X are extremely interesting to study since they are

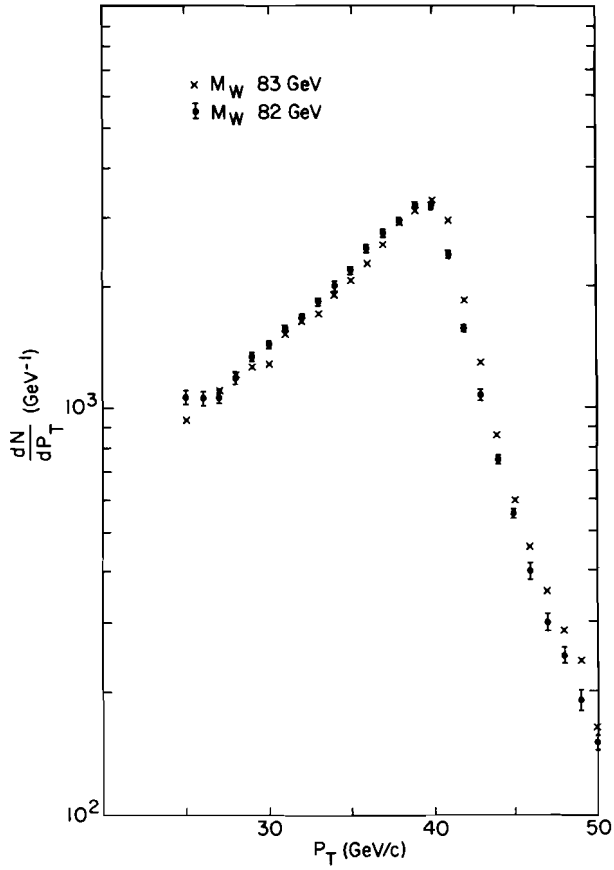

Fig. 4. Positron transverse momentum distributions for $W^+ \to e^+\nu$ decays with different values for the W mass

measures of the self-couplings present in any gauge theory. One would like not only to observe these processes but also to show that the couplings have the form predicted by the standard model.

These processes are difficult to measure experimentally. The rates are low and the potential real physics backgrounds are large. We have considered the problem of observing the reaction $pp \to W^{\pm} + \gamma + X$ and the background to be expected from $pp \to W^{\pm}$ + jet + X production. The $W^{\pm}$ is assumed to be detected via its leptonic decay $W^{\pm} \to e^{\pm} + \nu$ as discussed in the previous section and the single photon is then searched for in the selected $W^{\pm}$ event sample. We have not considered, for example, the possibility of triggering on an electron shower plus an isolated photon shower.

The detector used to simulate the experiment is similar to that used in the previous section for studying $W^{\pm}$ production. It covers the full azimuth ($\Delta\phi = 2\pi$) and $\Delta y = \pm 2$ (i.e. a 15° beam cone is excluded). Both the electromagnetic and hadronic calorimeters are segmented in towers pointing to the interaction point. Each tower covers 5° in θ and 9° in ϕ for a total of 1200 towers. For the present study the detection efficiency is assumed to be 100% once a track is within the geometrical acceptance of the detector. In addition no resolution or smearing effects are considered; the energy of each track is assumed to be contained in the tower to which it points. In principle this detector has a magnetic field so one might assume that for many tracks the hadron energy is determined from momentum measurement.

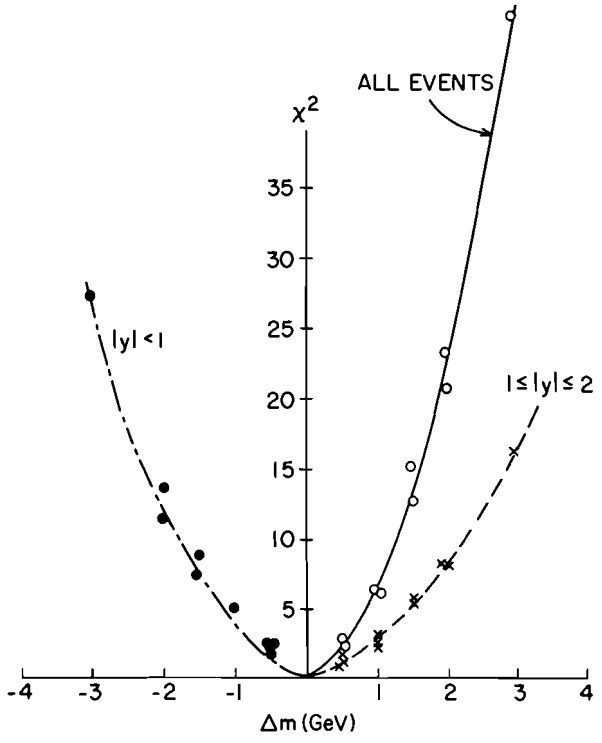

Fig. 5. Variation in χ^2 as a function of the change in W^+ mass for various $|y_e|$ cuts. Only one arm of the symmetric curves is drawn to clarify the plot.

Events were generated using the ISAJET Monte Carlo[2] program and the tracks projected into the detector described above. The pp → $W^\pm$ + γ + X cross section of Brown et al.[4] was used and for the $W^\pm$ decay, the angular averaged polarization computed by Brown was employed. The total cross section for P(γ) > 5 GeV/c at $\sqrt{s}$ = 800 GeV is ≈ 4×10^{-35}cm^2. We have considered only events with $P_T(\gamma) > 10$ GeV/c since it is unlikely that one would be able to effectively isolate the $W^\pm$ signal for lower values of the transverse momentum.[10] The effective pp → $W^\pm$+ γ + X cross section with $P_T(\gamma) > 10$ GeV/c is ≈ 4×10^{-36}cm^2. Since the branching ratio $W^\pm \to e^\pm$ + ν is calculated to be 8.5%, and ≈ 80% of the generated events have both the $e^\pm$ from the $W^\pm$ decay and the single γ within the detector acceptance, a total of 2720 pp → W^+ + γ + X events will be observed in an experiment with integrated luminosity L = 10^{40}cm^{-2}.

The primary physics background comes from pp → $W^\pm$ + jet + X events where the jet fragments contain a very high transverse momentum π°. We have generated background events in the range $10 \leq P_T(W^+) \leq 100$ GeV/c.[11] The total cross section for pp → $W^\pm$ + jet + X with $P_T(W^+) > 10$ GeV/c and $W^\pm \to e^\pm$ + ν is ≈ 8×10^{-35}cm^{-2}. This is 240 times the corresponding rate for $W^\pm$ + γ + X production.[12] The problem now is to evaluate how often this jet will emulate an "isolated" gamma. First we define a gamma candidate to be a tower with electromagnetic energy (EELEC) such that the transverse electromagnetic momentum for the tower is above the selected P_T cut. In addition we require that the total energy (ETOT) is not more than 25% higher than the electromagnetic energy (ETOT/EELEC < 1.25). This cut is intended to remove all towers with significant hadronic energy while at the same time allowing some reasonable energy accumulation for event overlaps due to the high luminosity (L = 10^{33}cm^{-2}sec^{-1}) used in the experiment. Approximately 3.4% of the jet events have both a tower passing the defined "gamma" cuts and the e^+ from the $W^\pm$ decay within the detector acceptance (Table II).

Table II
Effect of Cuts on Background and Signal for
$P_T(\gamma\text{-cell}) > 10$ GeV/c.

	$W^\pm+\gamma+X$	$W^\pm$+jet+X
$\sigma(P_T(W)>10$ GeV/c)	.28pb	79pb
$e^\pm$,"γ" both detected		
P_T("γ")>10GeV/c	.22pb	2.7pb
Largest P_T in cells surrounding the "γ" cell<1GeV/c	.22pb	.55pb
Opening angle between γ's in "γ"-cell<20mr	.22pb	.30pb
Opening angle between γ's in "γ"-cell<10mr	.22pb	.09pb

The angular correlation between the e^+ and gamma for the signal (Fig. 6) is quite similar to that for the $e^\pm$ and jet gamma candidate from the background (Fig. 7). However in many ways the signal and background should differ. In particular the gamma in the signal events should be isolated from other tracks while the background "gammas" should have other jet fragments in association. This information can be used in two ways.

First we can require the triggered tower to be isolated. To do this we consider the eight cells surrounding the triggered cell. In principle one could simply count the number of tracks. However this suffers from event overlap problems due to the high luminosity. A reasonable alternative is to consider the energy, or more effectively, the transverse momentum in the surrounding cells. To reduce the effects of energy pile-up we select the surrounding cell with the highest transverse momentum (P_{TMAX}). Essentially no signal events are removed if we require $P_{TMAX} < 1$ GeV/c. On the other hand only 15% of the $W^\pm$ + jet + X events survive the cut (Table II, Fig. 8).

Secondly we can consider in detail the contents of the triggered cell. For the pp → $W^\pm$ + γ + X signal the cell contains only a single high energy photon with the momentum distribution shown in Fig. 9. The background events on the other hand have complex structure since in general the cell energy is the sum of many jet fragments. The distribution of tracks in the selected cell is shown in Table III and the actual photon momentum distribution in Fig. 10. Since we have already excluded cells with significant hadronic energy in defining gamma candidates only 25% of the selected cells have hadron tracks. Consequently requiring no hadron track pointing into the cell provides little background rejection. On the other hand the electromagnetic energy is in general a composite of a number of photons (Table III). The question of whether or not one can resolve the multiphotons in the cell is difficult to answer in detail. However it seems reasonable to assume that if the vertices of the photon conversions are separated by more than a certain distance one will be able to tell that more than one photon was present. For example if 2 photons separated by 10mr (1cm at 1m) can be resolved, then only ≈ 15% of the background events survive as single photon candidates and the final ratio of signal to background is 2:1 (Table II). If one can only resolve photons with a 20mr opening angle, then the signal and background are comparable.

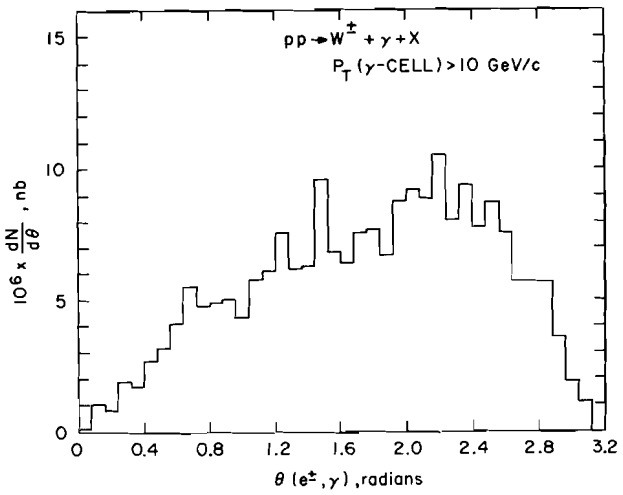

Fig. 6. Angular correlation between the e^+ and γ tracks for $pp \to W^{\pm} + \gamma + X$ events.

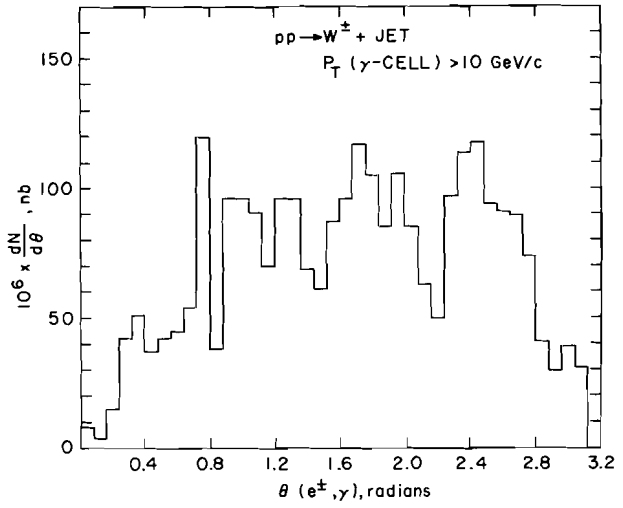

Fig. 7. Angular correlation between the e^+ and "γ" tracks for $pp \to W^{\pm}$ + jet + X events.

The signal to background ratio is comparable if a higher P_T cut is used but there is a loss of signal. We have considered a similar analysis to that described above with the cut at $P_T > 20$ GeV/c. The results are shown in Table IV, Fig. 12 and indicate again that a background level comparable to the signal can be attained.

It seems clear that one will be able to measure the rate for $pp \to W^{\pm} + \gamma + X$. However it remains to be seen how well one can test the various model predictions for this process. In particular for the standard model the $u\text{-}W^+$ angular distribution has a zero at + 1/3 whereas in non-standard models this angular distribution becomes almost uniform.

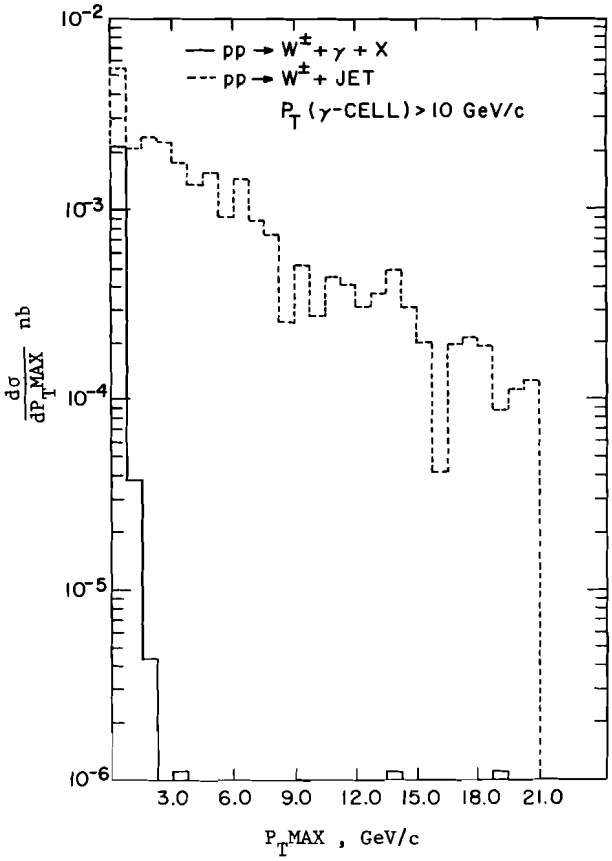

Fig. 8. Distribution of the maximum transverse momentum in the cells around the triggered γ-cell.

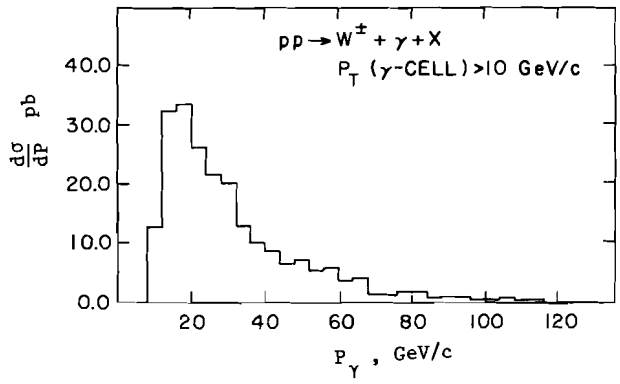

Fig. 9. Momentum distribution of γ's in the $pp \to W^{\pm} + \gamma + X$ events.

Table III
Particle Content of Cells from $pp \to W^{\pm}$ + jet events Satisfying the "γ"-Selection Criteria.

% of Cells With	Charged Particles	Photons	All Particles
0	84.0%	0	0
1	14.2%	14.3%	12.3%
2	1.3%	55.9%	50.3%
3	.5%	12.4%	16.4%
4	--	10.0%	10.8%
≥ 5	--	7.4%	10.2%

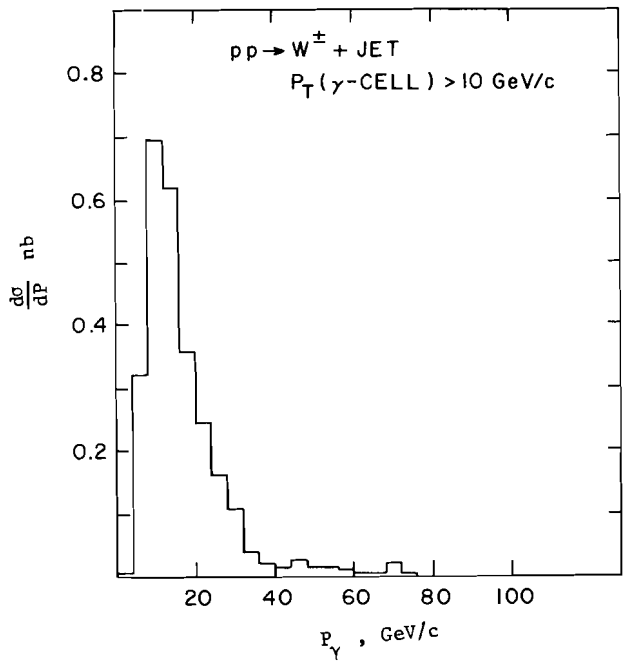

Fig. 10. Momentum distribution of γ's in the triggered tower in the pp → $W^{\pm}$ + jet + X events.

Table IV
Effect of Cuts on Signal and Background for
$P_T(\gamma\text{-cell}) > 20$ GeV/c

	$W^{\pm}+\gamma+X$	$W^{\pm}$jet+X
$\sigma(P_T(W)>10\text{GeV/c})$	.28pb	79pb
e,"γ"both detected P_T("γ")>20GeV/c	.056pb	.43pb
Largest P_T in cells surrounding the "γ" cell<1 GeV/c	.056pb	.076pb
Opening angle between γ's in "γ"-cell<20mr	.056pb	.055pb
Opening angle between γ's in "γ"-cell<10mr	.056pb	.046pb

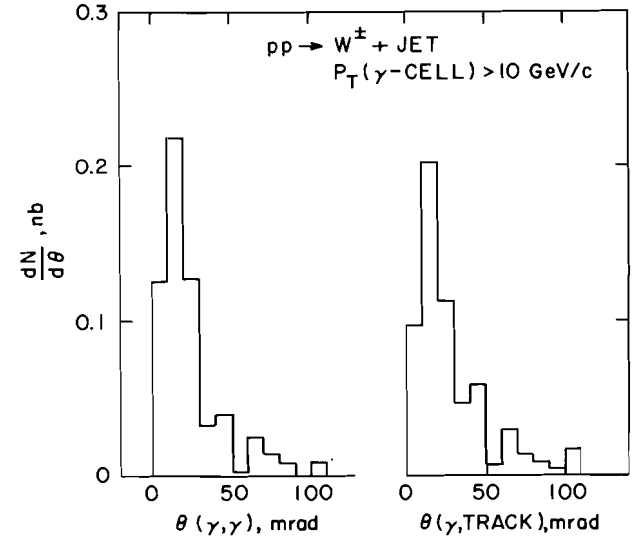

Fig. 11. Distribution of the largest opening angle between the fastest γ in the triggered tower and a) other γ's in the tower; b) all other tracks in the tower.

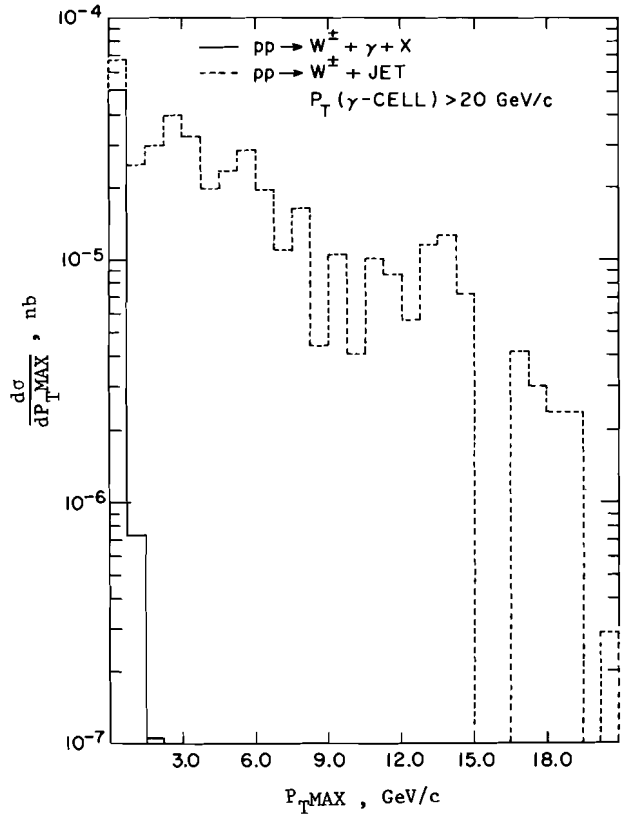

Fig. 12. Distribution of the maximum transverse momentum in the cells around the triggered γ-cell.

IV. Polarized Beams in the Colliding Beam Accelerator

Introduction

The AGS will have polarized beams by 1984. These polarized beams can be injected into the CBA. Polarization is maintained during acceleration by a spin rotation trick that automatically corrects for depolarizing effects by averaging them to zero for one (or two) trips around the ring. This trick, called a Siberian Snake,[13] uses a string of warm magnets which easily fits into the ISABELLE lattice. Although snakes have not been tested yet, their use appears to be quite straight-forward. Courant gave a talk on their second-order effects at the Spin Physics Symposium, held at BNL in September 1982.

The polarization can be transverse or longitudinal. Helicity states are obtained by using a half-snake of magnets, followed by the experiment, followed by another half-snake, to bring the polarization back to transverse. With two snakes per ring, each interaction region would be fully polarized.[13] The maximum polarization would be ≈70%.

Luminosity

The luminosity at ISABELLE expected with the polarized AGS source presently being installed is a factor of 10-100 below the luminosity using unpolarized protons. However, there are at least two ways in the next few years to reach 10^{13} polarized protons per pulse in the AGS and full luminosity in a

CBA with polarized beams: using expected (in-hand) source improvements and stacking in a 200 MeV accumulator, or using an entirely new source (in development) of polarized atomic hydrogen to reach 10^{13} ppp directly. It is therefore reasonable to assume that the luminosity with polarized protons will be the same as with unpolarized protons and we do so in what follows.

Measuring Polarization and Polarization Reversal[14]

A 5% measurement of P in 1 minute can be done using the Coulomb-nuclear interference region where the p-p analyzing power can be calculated (it is a few %). Note that the precise polarization enters most physics results only as an overall normalization, independent of P_T or dilepton masses, for example.

Polarization reversal can be done by slowly reversing the fields in the snakes and can be done hourly. If box-car stacking is used, alternate cars can have opposite polarization, effectively eliminating systematic biases.

Statistical Significance of using Polarization to Study Weak Effects

Paige, Trueman and Tudron[15] calculated that with a 100% polarized proton beam, $\sigma_- \approx 3\sigma_+$. For a 70% polarized beam, $\sigma_- \approx 2\sigma_+$. ($\sigma_-$ is the cross section with both protons left-handed, σ_+ with both right-handed.) With a polarized beam available, one can

a) add the +,- helicities together giving the unpolarized result.
b) Use the subtraction $(\sigma_+ - \sigma_-)/(\sigma_+ + \sigma_-)$ to eliminate strong-interaction background with no assumptions about the background. One can do this bin-by-bin (say, in energy or P_T bins) to find the shape of the signal. The statistical signal is 1/1.5 smaller than the unpolarized case, but the background uncertainty is eliminated (more on this later).

If the background subtraction for the unpolarized case is done by interpolating between "background-only" regions on either side of an anomaly, typically one side has few events (for example, high P_T), so the background uncertainty is very large. Therefore a bin by bin subtraction, as described in b) above, is much more reliable, even though the two methods are in principle comparable statistically.

We have assumed an experimental set-up with 2π acceptance about 90°, ± 5 GeV mass resolution for the signal and an integrated luminosity of $10^{39}\,cm^{-2}$. An "experimental" background was generated by applying a Poisson distribution to the calculated background in 2.5 GeV bins. The total number of events is shown for masses between 65 and 90 GeV in Fig. 13, and it indicates how difficult it is to see a 10 GeV wide, 1% signal.

A fit of the form CM^{-p} (M is the dijet mass) to the background leaving out the signal had a χ^2 of about 40 for 9 degrees of freedom. When this fit is subtracted from the "data" the signal shows up very well (Fig. 14). To a large degree, this must be attributed to the simple form of the input background, which was also of the form CM^{-p}.

The polarized beams can be used to ensure that the background subtraction is done correctly, and no fitting is needed. The result of subtracting a run of right-handed polarized protons from one of left-handed

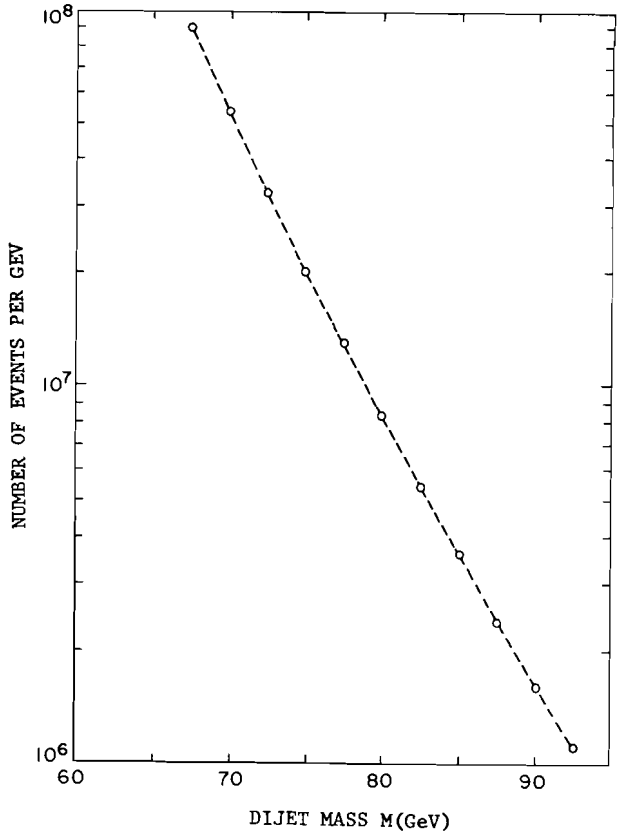

Fig. 13. Effective mass distribution for pairs of jets

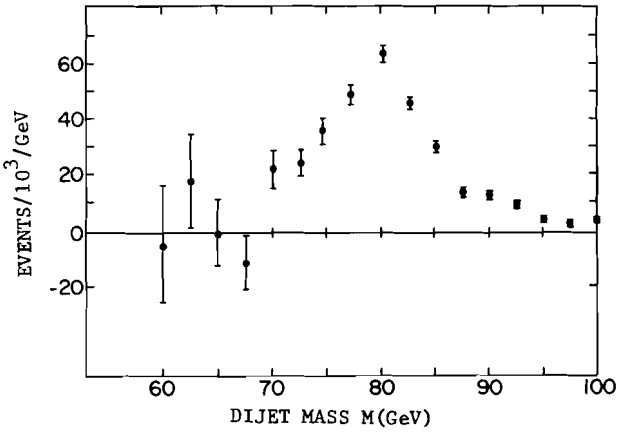

Fig. 14. Background subtracted effective mass distribution for pairs of jets. The background is determined from a fit to the distribution in Fig. 13 excluding the W region.

polarized protons, as described above, is shown in Fig. 15. The signal is quite clear. In Fig. 15 100% beam polarization is assumed. For 70% beam polarization the signal would be reduced by a factor of .7 while the background in the figure would be unaffected.

There are many other interesting experiments that can be carried out if polarized beams are available in

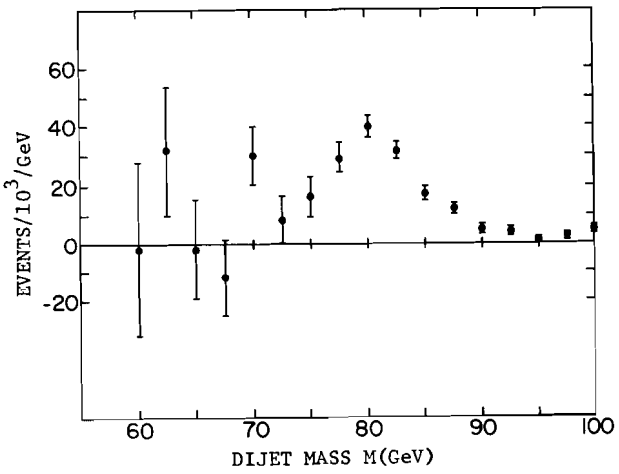

Fig. 15. Mass distribution of jet pairs obtained by subtracting bin by bin the distributions for each polarization.

the CBA. A whole range of weak effects can be separated by reversing the spin, just as in the case discussed above for extracting W → jets from the background. (These generally require only one beam to be polarized, but then the size of the effect drops by about a factor of two. This might be regained if there are luminosity gains by polarizing only one beam.)

Obviously, one can use this technique to verify and measure the magnitude of parity violation in W → e + ν or W → μ + ν. This would be a very strong clear signal. If a second, higher mass W were discovered this would be especially exciting because the second W could couple either to left- or right-handed currents, and the two cases are distinctly different in this regard.

Two spin effects (the dependence of cross sections on the relative polarization states of the initial proton beams) are a valuable QCD test, as has been analyzed in detail by Babcock, Monsay and Sivers.[16] Also one would like to extend experiments of the type carried out by Krisch's group at Argonne to higher energy and P_T.[17] Single-spin asymmetries are predicted by QCD to be zero, in leading order, but in view of the large hyperon polarization seen in lower energy experiments, which is not understood,[18] it would be very interesting to carry out the analogous experiment, looking at the dependence on initial state proton polarization. Obviously, the polarization of final state hyperons is another interesting experiment. The correlation of the hyperon polarization with initial polarization is an obvious case. Finally, Sivers[19] has pointed out that the two-spin asymmetry in pp → γ + X is sensitive to the spin dependence of the gluon structure functions.

V. High Luminosity

A few methods of improving the CBA luminosity above 10^{33} have been suggested. For example, if 2 in 1 magnets are used in the ring, a luminosity of 7 x 10^{33} may be possible. We have, therefore, studied the backgrounds and dead time problems that one could have in the MIT[1] high resolution muon detector at a luminosity of 10^{34}.

We find that the situation with high P_T muon triggers and with high P_T muon momentum measurement to be unchanged. Apart from the calorimeter we are in no way limited by singles rates and high P_T muons penetrating the calorimeter are still rare.

On the other hand the increase in luminosity does affect the calorimeter. Since our calorimeter is based on scintillator, we expect that with proper care we can use a 100 nsec gate width for energy integration. If a luminosity of 10^{34} were likely, we would then read out the calorimeter energy as a function of time allowing us to have a 30 nsec time window on the off-line energy sum.

One can use the new data from the SPS to estimate the total energy in the calorimeter in a 30 nsec window.

$$E_{tot} \approx 2\langle m_T\rangle L\, \sigma_{tot} \sinh(y_{max})\tau \langle \text{number/unit rapidity}\rangle$$

$$= 2\text{x}.5\ \text{GeV} \text{x} 10^{34}\ \text{cm}^{-2}\text{sec}^{-1} \text{x} 60\text{x}10^{-27}\text{cm}^2 1\text{x}30\text{x}10^{-9}\text{secx}5$$

$$= 90\ \text{GeV}$$

This comes from $\sigma_{tot} L\tau$ = 18 events, so that a typical fluctuation on that 90 GeV could be 25 GeV. This background of energy deposition in the calorimeter would decrease the effectiveness of cuts to reduce the background in the single high P_T muon spectrum due to heavy quark decay. We find, however, that the calorimeter would still be somewhat useful in reducing this background.

However in the high mass dimuon spectrum, no calorimeter cut is required. We therefore believe that at a luminosity of 10^{34} we would have no such difficulty searching for high mass muon pairs as might come from a higher mass Z°. This is the place where high luminosity is most important anyway. We also find that very high P_T single muons such as might come from a high mass $W^{\pm}$ could be seen above background. If the background from heavy quark decays were increased by a factor of more than 10 from present estimates, the single lepton measurement would no longer work without some additional background suppression such as the use of polarized beams to remove the parity conserving background. We could also still measure very high P_T QCD jet cross sections for P_T > 150 GeV. In short, the most interesting things that require high luminosity could still be done at 10^{34}. Some detailed study of intermediate P_T jets or standard $W^{\pm}$ production could be done in lower luminosity runs at ≈ 10^{33} $\text{cm}^{-2}\text{sec}^{-1}$.

High Mass Z°'s

The couplings of multiple Z°'s are completely undetermined. Therefore the production cross section and widths are very model dependent. Some assumption must be made to quantify the sensitivity of a CBA experiment to higher mass Z°'s. A reasonable assumption is that the higher mass Z° has the same dimensionless coupling constant as does the standard Z_o. In Weinberg-Salam for example, g and g' differ by only a factor of 2 according to the measured value of $\sin^2\theta_w$.

If we assume that the new Z couples with the same strength as the standard W-S Z°, then we find that

$$\Gamma_{Z'} = \frac{m'}{m}\Gamma_Z$$

and

$$\sigma_{tot_{Z'}} = (m/m')^2 \frac{F(m'^2/s)}{F(m^2/s)} \sigma_{tot_Z}$$

where F can be estimated from the Drell-Yan continuum,

$$F = m^3 \frac{d\sigma}{dmdy} \Big| \; y = 0.$$

This is just a factor of m different from the Drell-Yan scaling law (Fig. 16,17) and, in fact, because the width increases linearly with m, $d\sigma/dm$ at the peak follows Drell-Yan scaling exactly. From this it is easy to calculate limits on Z masses which are visible under various luminosity assumptions. These are shown in the following table as the limiting mass to get 100 events in a 10^7 sec experiment.

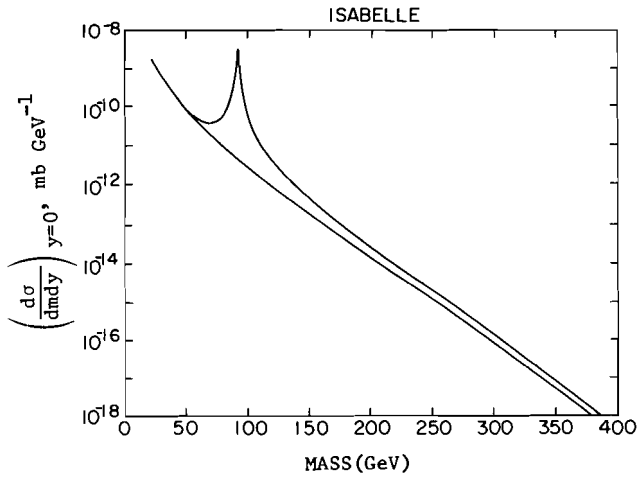

Fig. 16. Drell-Yan continuum and Z° cross section for a pp collider with $\sqrt{s}$ = 800 GeV.

Table V
Z° Mass Limits for Different Energy and Luminosity Machines

	L	M Zmax
pp	CBA $10^{34}/cm^2/sec$	320 GeV
pp	CBA $10^{33}/cm^2/sec$	260 GeV
$\bar{p}p$	FNAL $10^{30}/cm^2/sec$	210 GeV
$\bar{p}p$	FNAL $10^{29}/cm^2/sec$	110 GeV

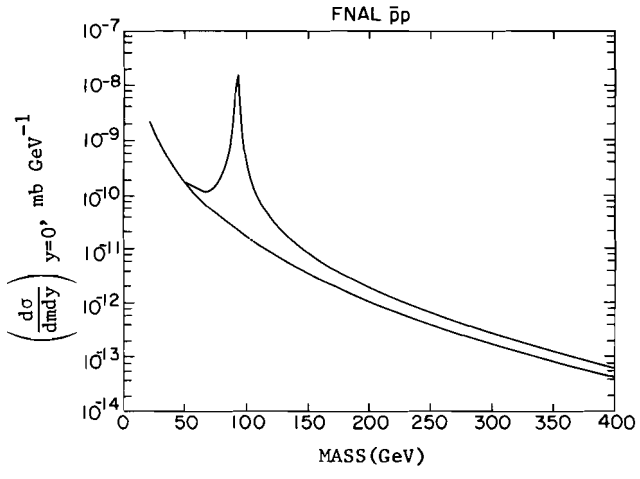

Fig. 17. Drell-Yan continuum and Z° cross section for a $\bar{p}p$ collider with $\sqrt{s}$ = 2000 GeV.

This research supported by the U.S. Department of Energy under contract DE-AC02-76CH00016.

References

1. MIT DETECTOR see e.g.
   A personal view of the ISABELLE Project, S.C.C. Ting, BNL, 51443; (1981) ISABELLE: Proceedings of the 1981 Summer Workshop pp. 334 - 401; Report of Z°, $W^{\pm}$, γ Working Groups, M. Chen et al. ibid, pp. 448 - 474.
2. ISAJET, F.E. Paige and S.D. Protopopescu, BNL29777 (1981).
3. F.E. Paige, Updated Estimates of W production in pp and pp interactions. Topical Workshop on the production of new particles in Super High Energy Collisions, Madison, Wisconsin, Oct. 22-24, 1979.
4. R.W. Brown, D. Sahdev, K.O. Mikaelian, Phys. Rev. D20, 1164 (1979).
5. See for example, Ref. 3.
6. J.F. Owens, E. Reya, M. Gluck, Phys. Rev. D18, 1501 (1948).
7. M. Banner et al. CERN EP/82-62 Subm. to Phys. Lett.
8. F.E. Paige, Monte Carlo simulation of Heavy Quark production in pp and pp reactions. Proton-Antiproton Collider Physics - 1981, Madison, Wisconsin, Edited by V. Barger, D. Cline, F. Halzen, AIP, New York 1982.;
   M. Chen et al. ISABELLE Proceedings of the 1981 Summer Workshop, pp. 447 - 473, H.A. Gordon, Editor, BNL Aug. 1981.
9. F. Halzen, A.D. Martin, D.M. Scott, Phys. Rev. D25, 754 (1982).
10. With $P_T \geq 10$ GeV/c the observed P_T distribution for the e^+ from the $W^{\pm}$ decay peaks at ≈ 30 GeV/c. From the discussion in the previous section on W^+ detection it is possible to isolate an acceptable W^+ signal in this region.
11. All signal events corresponding to a total integrated luminosity of ≈ 10^{40} cm^{-2} were generated. A total of 11,000 background events were generated. This would be the yield for an integrated luminosity of only ≈ 10^{38} cm^{-2}. Consequently, the statistical accuracy for some of the data when higher P_T cuts are made is not very good. In addition since one is dealing with the tails of the Monte Carlo distribution caution should be exercised in interpreting the conclusions reached.
12. This ratio is expected to be
$$\approx \frac{\alpha_s}{\alpha} \frac{\langle g(x) \rangle}{\langle \bar{q}(x) \rangle} \approx \frac{10x3(1-x)^5}{.15(1-x)^7} \approx 200$$
since x ≈ .1 at the CBA.
13. E.D. Courant, Proceedings of the 1980 International Conf. on High Energy Physics with Polarized Beams and Polarized Targets, Lausanne, 1980, p. 102.
14. See 1981 ISA Summer Workshop Proceedings, p. 600.
15. Frank E. Paige, T.L. Trueman and Thomas N. Tudron, Phys. Rev. D19, 35 (1979).
16. T. Babcock, E. Monsay and D. Sivers, Phys. Rev. D19, 1483 (1979).
17. See Ref. 13, p. 545.
18. See Ref. 13, p. 114 and p. 141.
19. D Sivers, private communication.